Molecular Therapy
Nucleic Acids
Original Article

Exosomes from *SIRT1*-Overexpressing ADSCs Restore Cardiac Function by Improving Angiogenic Function of EPCs

Hui Huang,[1,4] Zhenxing Xu,[1,4] Yuan Qi,[1] Wei Zhang,[1] Chenjun Zhang,[1] Mei Jiang,[2] Shengqiong Deng,[3] and Hairong Wang[1]

[1]Department of Cardiology, Shanghai Pudong New Area Gongli Hospital, Shanghai 200135, P.R. China; [2]Department of Neurology, Shanghai Pudong New Area Gongli Hospital, Shanghai 200135, P.R. China; [3]Department of Clinical Laboratory, Shanghai Pudong New Area Gongli Hospital, Shanghai 200135, P.R. China

Acute myocardial infarction (AMI) is one of the leading causes of mortality in cardiovascular diseases. The aim of this study was to investigate whether exosomes from Sirtuin 1 (*SIRT1*)-overexpressing adipose-derived stem cells (ADSCs) had a protective effect on AMI. The expression of C-X-C chemokine receptor type 7 (CXCR7) was significantly downregulated in peripheral blood endothelial progenitor cells (EPCs) from AMI patients (AMI-EPCs) compared with that in healthy donors, which coincided with impaired tube formation. The exosomes from SIRT1 overexpression in ADSCs (ADSCs-SIRT1-Exos) increased the expression of C-X-C motif chemokine 12 (CXCL12) and nuclear factor E2 related factor 2 (Nrf2) in AMI-EPCs, which promoted migration and tube formation of AMI-EPCs, and overexpression of CXCR7 helped AMI-EPCs to restore the function of cell migration and tube formation. Moreover, CXCR7 was downregulated in the myocardium of AMI mice, and knockout of CXCR7 exacerbated AMI-induced impairment of cardiovascular function. Injection of ADSCs-SIRT1-Exos increased the survival and promoted the recovery of myocardial function with reduced infarct size and post-AMI left ventricular remodeling, induced vasculogenesis, and decreased AMI-induced myocardial inflammation. These findings showed that ADSCs-SIRT1-Exos may recruit EPCs to the repair area and that this recruitment may be mediated by Nrf2/CXCL12/CXCR7 signaling.

INTRODUCTION

Acute myocardial infarction (AMI) is a myocardial necrosis caused by acute coronary artery and persistent ischemia and hypoxia, which has a high mortality rate.[1] In recent years, it has been reported that adipose-derived stem cell (ADSC) transplantation is an effective treatment for the pathophysiology of AMI.[2] Early studies have shown the multi-differentiation potential of ADSCs, such as their ability to differentiate into cardiomyocytes, vascular endothelial cells, and vascular smooth muscle cells.[3,4] However, subsequent studies have failed to reproduce this significant differentiation of ADSCs, because transplanted ADSCs have poor survival in the inflammatory and ischemic microenvironments of AMI.[5,6] Furthermore, studies have shown that ADSCs promote angiogenesis and repair damaged myocardial tissue by the secretion of paracrine factors.[7,8] We, therefore, speculated that paracrine factors secreted by ADSCs play an important role in the repair and regeneration of heart tissue.

Exosomes are vesicles secreted by various types of cells, with a diameter of 30–100 nm. They are widely distributed in body fluids and contain proteins, lipids, nucleic acids, and other contents.[9] Studies have confirmed that exosomes play a wide range of roles, involving cell signaling, cell differentiation, immune regulation, substance metabolism, gene regulation, tumor cell growth, and other processes.[10,11] Xu et al.[12] showed that exosomes from ADSCs can stimulate most myocardial protective factors; inhibit myocardial cell apoptosis; promote angiogenesis; and, thus, improve cardiac function and protect myocardium. However, the exact mechanism of exosomes from ADSCs in myocardial protection of AMI has not been fully elucidated.

Silencing information regulator factor 1 (*SIRT1*), a histone deacetylase, plays an important role in cell metabolism, cell survival, cell senescence, DNA repair, cell proliferation, differentiation, apoptosis, inflammation, and other physiological and pathological processes.[13,14] *SIRT1* is reported to be involved in controlling many processes such as aging, osteoporosis, diabetes, and cardiovascular disease.[15,16] Studies have shown that *SIRT1* is involved in myocardial injury during diabetes.[17] It has also been reported that overexpression of *SIRT1* in mesenchymal stem cells promotes dentin formation[18] and protects against bone defects[19] and that activation of the *SIRT1* pathway improves survival of ADSCs.[20] However, whether exosomes from ADSCs overexpressing *SIRT1* promote angiogenesis and myocardial repair of AMI has not been reported.

Received 31 March 2020; accepted 6 July 2020;
https://doi.org/10.1016/j.omtn.2020.07.007.

[4]These authors contributed equally to this work.

Correspondence: Hairong Wang, Department of Cardiology, Shanghai Gongli Hospital, The Second Military Medical University, 219 Miao-Pu Road, Shanghai 200135, P.R. China.
E-mail: hairong19@yahoo.com

Oxidative stress can be induced by both ischemic hypoxia and post-ischemic reperfusion in local tissues during myocardial infarction. It has been reported that *SIRT1* may regulate oxidative stress and antioxidant enzymes.[21] Nuclear factor E2 related factor 2 (*Nrf2*) is an important antioxidant factor. A study has shown that activation of the SIRT1/Nrf2 pathway alleviated myocardial ischemia/reperfusion injury.[22] We, therefore, hypothesized that exosomes from ADSCs overexpressing *SIRT1* could promote myocardial functional repair of AMI by activating *Nrf2*.

Endothelial progenitor cells (EPCs) are involved not only in embryonic angiogenesis but also in the formation of new blood vessels after birth.[23] The EPC content in peripheral circulation is small. Although EPCs can be mobilized after the occurrence of AMI, they are far from enough to meet the needs of repair. Moreover, common complications of coronary heart disease, such as diabetes, hypertension, and lipid metabolic disorders, severely weaken their ability to mobilize homing and angiogenesis.[24] Fish *et al.*[25] showed that exosomes from ADSCs enhanced the homing ability of EPCs and promoted angiogenesis to repair myocardial functions. Stromal cell-derived factor 1 (SDF-1), also known as C-X-C motif chemokine 12 (CXCL12), is a key chemokine that regulates the transport of hematopoietic stem cells between the bone marrow and peripheral blood circulation and attracts EPCs to the ischemic region. C-X-C chemokine receptor type 4 (CXCR4) was once considered to be the only CXCL12 receptor, and many studies have shown that the CXCL12/CXCR4 axis plays a role in the mobilization of stem cells and EPCs from the bone marrow to target tissues; it also plays a role in chemotaxis, adhesion, and angiogenesis.[26] CXCR7 is the second CXCL12 receptor discovered in recent years, and its affinity with CXCL12 is 10 times greater than that of CXCR4.[27] Zhang *et al.*[28] found that the expression of CXCR7 in EPCs of hypertensive patients was low, which led to a decrease in *in vitro* function and *in vivo* re-endothelialization of EPCs of hypertensive patients. In the present study, EPCs were isolated from the peripheral blood of AMI patients and healthy subjects, and the AMI model was constructed using CXCR7 knockout mice to study whether the exosomes from ADSCs overexpressing SIRT1 could promote the homing of EPCs and thereby promote myocardial functional repair.

RESULTS

AMI Reduced the Expression of CXCR7 in EPCs and Decreased the Angiogenesis Function of EPCs

As shown in Figure 1A, EPCs surface markers were examined by flow cytometry, which showed that peripheral blood EPCs in healthy subjects (controls) and AMI patients were positive for the CD34 and CD133 surface markers and negative for CD45. To determine how EPCs were affected by AMI, we detected the expression of the CXCL12 receptor, CXCR7, in peripheral blood EPCs of both healthy subjects and AMI patients, as well as the tube formation capacity of EPCs. The expression of CXCR7 in the EPCs of AMI patients (AMI-EPCs) was significantly lower than that of healthy subjects (Figures 1B and 1C; $p < 0.05$). Compared with the EPCs of healthy subjects, the length of tubes formed by AMI-EPCs was significantly shorter, which indicated a functional deficiency (Figures 1D and 1E; $p < 0.01$).

Exosomes from ADSCs Promoted EPC Migration and Tube Formation, and Upregulation of CXCR7 Helped Restore the Function of AMI-EPCs

To determine whether ADSC exosomes and the CXCL12 receptor, CXCR7, were involved in the chemotaxis and tube formation of EPCs, EPCs from healthy subjects (control-EPCs) were transiently transfected with lentiviral small interfering RNA (siRNA) control plasmid or small interfering *CXCR7* (si*CXCR7*) plasmid, while AMI-EPCs were transfected with lentiviral vector control (vector) or overexpressed *CXCR7* vector (Lv-*CXCR7*) for 48 h. Isolated ADSCs were labeled with different cell-surface marker antibodies to determine the cell phenotype. Figure S1 shows that ADSCs were positive for the CD90 and CD29 mesenchymal cell markers. CXCR7 protein levels were also analyzed in all cells using western blotting (Figure 2A). Control-EPCs transfected with si*CXCR7* showed a significant decrease in CXCR7 compared with the non-transfected control-EPCs ($p < 0.01$), and AMI-EPCs transfected with the Lv-*CXCR7* showed a significant increase in CXCR7 expression, as expected, compared with the non-transfected AMI-EPCs ($p < 0.01$; Figure 2B).

To analyze the chemotaxis of control-EPCs transfected with siRNA or si*CXCR7* and AMI-EPCs transfected with lentiviral vectors or Lv-*CXCR7* (upper chamber), the cells were cultured in Transwell chambers with ADSCs with or without GW4869 (lower chamber) for 24 h (Figure 2C). The results showed that the migration ability of EPCs co-cultured with ADSCs was significantly improved, compared with that of the Dulbecco's Modified Eagle's Medium (DMEM) group ($p < 0.05$). The increase in ADSC response was almost completely blocked when control-EPCs were transfected with si*CXCR7* or ADSCs pretreated with GW4869 ($p < 0.05$, Figure 2D).

For the tube formation assays, different transfected control-EPCs and AMI-EPCs were cultured for 48 h with cell-culture supernatants of ADSCs with or without GW4869 (Figure 2E). The same trend was seen for tube formation assays as was seen for the chemotaxis of EPCs (Figure 2F). These results indicated that exosomes from ADSCs and CXCR7 were important for the recruitment and tube formation of EPCs.

Direct Transfer of SIRT1 from ADSCs to EPCs Using Exosome Delivery

We used lentiviral overexpression of *SIRT1* plasmids to transfect ADSCs (Figure S2), and exosomes were isolated from ADSCs or ADSCs overexpressing *SIRT1* and then were characterized by transmission electron microscopy, nanoparticle tracking analysis, and western blotting. Electron micrographs showed that the collected products had a spheroid morphology (Figure 3A); the size distribution ranged from 80 to 120 nm (Figure 3B). The

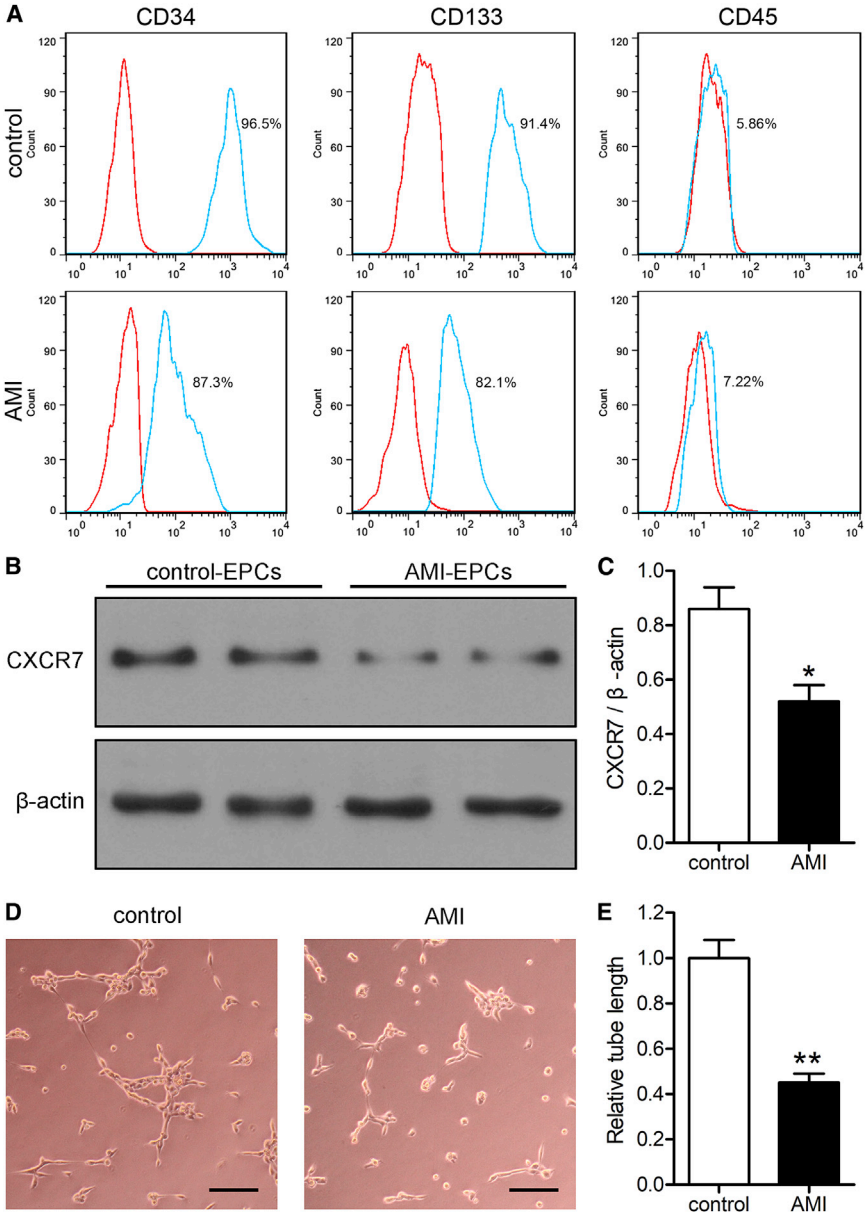

Figure 1. AMI Reduced the Expression of CXCR7 in EPCs and Decreased the Angiogenesis Function of EPCs

(A) Flow cytometry analysis of the expression of CD34/CD133/CD45 (green lines) in the peripheral blood EPCs of healthy subjects (control) and AMI patients, which were compared with isotype controls (red lines). (B) Expression of CXCR7 of EPCs was detected by western blots. (C) The western blot results were normalized to β-actin. *$p < 0.05$, compared to the control group. (D) The angiogenic function of EPCs was evaluated by tube formation assays. Scale bars, 100 μm. (E) The tube lengths were measured, and the control-EPCs were normalized to 1. **$p < 0.01$, compared to the control group.

results of western blotting showed that overexpression of *SIRT1* increased the protein expression level of SIRT1 in exosomes more than that in non-transfected control ADSCs, and specific exosome surface proteins (CD63 and TSG101) were found in the exosomes of both ADSCs (ADSCs-Exos) and *SIRT1*-overexpressed ADSCs (ADSCs-SIRT1-Exos), while they were almost undetectable in ADSCs (Figure 3A). To determine whether the exosomes could be taken up by EPCs, PKH26-labeled exosomes were incubated with AMI-EPCs for 24 h. Fluorescent microscopic imaging showed that ADSCs-Exos were found in AMI-EPCs (Figure 3D). To further determine whether SIRT1 was directly transferred from ADSCs to AMI-EPCs, exosomes were isolated from ADSCs or ADSCs, which had been transfected with green fluorescent protein (GFP)-labeled SIRT1, and were added to AMI-EPCs. Confocal microscopy showed fluorescently labeled signals in the AMI-EPCs incubated with exosomes obtained from cells transfected with GFP-labeled SIRT1 (Figure 3E), confirming that SIRT1 was transferred from ADSCs to AMI-EPCs via exosomes.

Exosomes from ADSCs Overexpressing *SIRT1* Restored AMI-EPC Migration and Tube Formation involving Nrf2 Activation and CXCL12 Secretion

To investigate whether ADSCs-SIRT1-Exos enhanced the migration ability and angiogenesis of AMI-EPCs, AMI-EPCs were pretreated with ADSCs-Exos or ADSCs-SIRT1-Exos. The results showed that the migration ability of AMI-EPCs pretreated with ADSCs-Exos was significantly improved, compared with that of the untreated group ($p < 0.05$). Moreover, the highest migration ability was observed in the ADSCs-SIRT1-Exo group among the three groups (Figures 4A and 4B). The same trend was seen for angiogenesis assays as that for the migration ability of AMI-EPCs (Figures 4C and 4D). In contrast, pretreatment with ADSCs-siSIRT1-Exos did not affect the migration and angiogenesis abilities of AMI-EPCs (Figure S3).

It has been reported that high expression of CXCR7 enhanced the angiogenic function of EPCs by enhancing the activity of Nrf2.[29] To investigate whether Nrf2 and CXCL12 were involved in the effects of ADSCs-SIRT1-Exos, the expressions of Nrf2 and CXCL12 in AMI-EPCs were detected by western blotting. The results showed that ADSCs-SIRT1-Exo treatment significantly increased the levels of Nrf2 and CXCL12 in AMI-EPCs when compared with the untreated group ($p < 0.01$; Figures 4E–4G). To determine the potential molecular mechanism of SIRT1 inducing Nrf2 protein expression

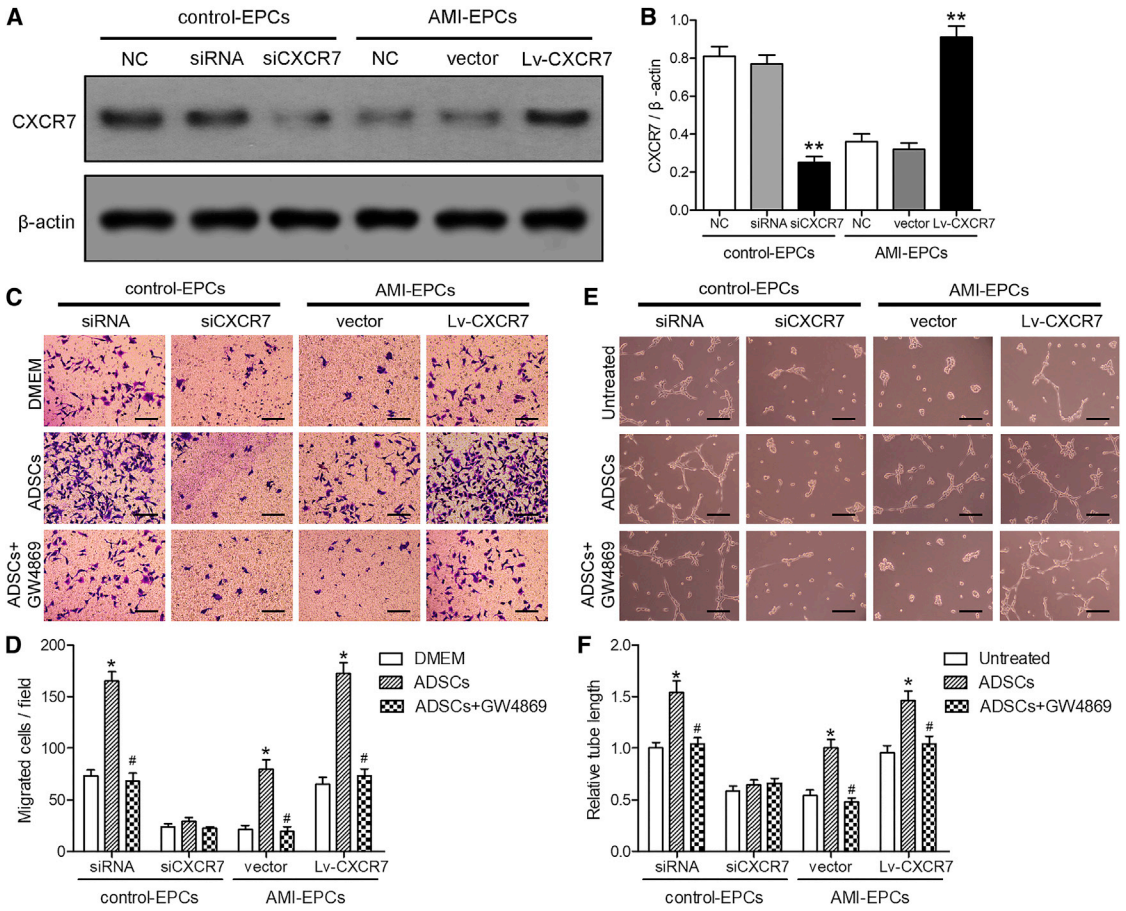

Figure 2. Exosomes from ADSCs Promoted EPC Migration and Tube Formation, and Upregulation of CXCR7 Helped AMI-EPCs Restore Cell Migration and Tube Formation

(A and B) EPCs from healthy controls (control-EPCs) were transfected with interfering plasmid or lentiviral interfering CXCR7 plasmid, while EPCs from acute myocardial infarction (AMI) patients (AMI-EPCs) were transfected with lentiviral plasmid or lentiviral overexpression of the CXCR7 plasmid, and cultured for 48 h. (A) Expression of CXCR7 was detected by western blotting. (B) The western blot results were normalized to β-actin. $^{**}p < 0.01$, compared to the non-transfected cells of control- or AMI-EPCs. (C) Cell migration was measured using Transwell assays. The upper chamber contained EPCs; the lower chamber contained DMEM containing 10% FBS or ADSCs with or without pretreatment with 2.5 μM GW4869 for 8 h. Scale bars, 100 μm. (D) Migrated cells were calculated. $^{*}p < 0.05$, compared to the DMEM control group; $^{\#}p < 0.05$, compared to the ADSC-treated group. (E and F) The indicated EPCs treated with supernatants of ADSCs with or without pretreatment with GW4869. (E) The tube formation assay. Scale bars, 100 μm. (F) The tube lengths were measured. The control-EPCs transfected with siRNA were normalized to 1. $^{*}p < 0.05$, compared to the untreated group; $^{\#}p < 0.05$, compared to the ADSCs-supernatant-treated group.

in AMI-EPCs, we assessed the levels of acetylated Nrf2 by immunoprecipitation. Figure 4H shows that ADSCs-SIRT1-Exo treatment led to the deacetylation of Nrf2, indicating that Nrf2 served as a direct substrate of SIRT1 in AMI-EPCs. Together, these results indicated that ADSCs-SIRT1-Exos promoted the recruitment and tube formation of the AMI-EPCs involved in upregulating expressions of Nrf2 and CXCL12.

Injection of Exosomes from ADSCs Overexpressing SIRT1 Helped Restore Cardiac Function in the AMI of Wild-Type (WT) Mice but Not in CXCR7 Knockout Mice

The levels of CXCR7 were measured in myocardial tissues of mice at 28 days after AMI or sham surgery to investigate the relationship between CXCR7 and AMI. Western blotting showed that the CXCR7 levels of AMI mice were significantly lower than those of sham-surgery mice (Figure 5A). Next, we investigated whether *CXCR7* knockout ($CXCR7^{-/-}$) mice had an effect on cardiac function in response to AMI. CXCR7 expression was confirmed in WT and $CXCR7^{-/-}$ mice by western blotting (Figure 5B). Kaplan-Meier survival analysis showed that injection of ADSCs-SIRT1-Exos into WT mice had significantly better results after AMI than injection of vehicle or ADSCs-Exos into mice (Figure 5C). We measured the cardiac function of WT and $CXCR7^{-/-}$ mice subjected to AMI for 28 days after injection of phosphate-buffered saline (PBS; vehicle), ADSCs-Exos, or ADSCs-SIRT1-Exos (Figure S4). The AMI-induced high left ventricular enddiastolic dimension (LVEDD), and left

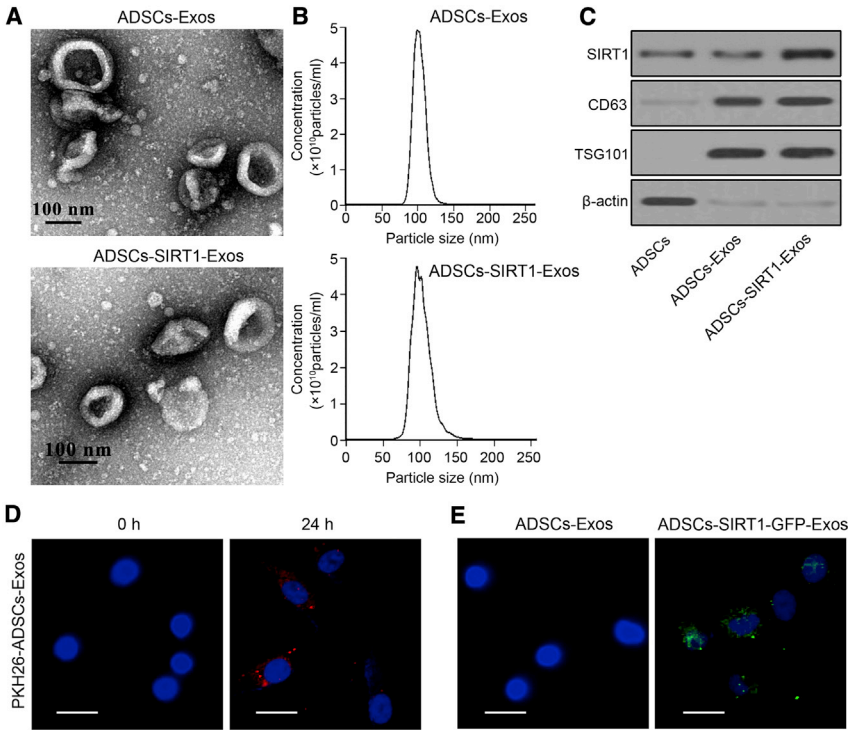

Figure 3. Direct Transfer of SIRT1 from ADSCs to EPCs Using Exosome Delivery

(A) Transmission electron microscopy of exosomes from ADSCs (ADSCs-Exos group) or ADSCs overexpressing SIRT1 (ADSCs-SIRT1-Exos group). Scale bars, 100 nm. (B) Nanoparticle tracking analysis of the exosome diameters (in nanometers). (C) Expression of SIRT1 and specific exosomal surface markers (CD63 and TSG101) were detected by western blotting of ADSCs and exosomes. (D) Localization of PKH26-labeled ADSCs-Exos (red) in AMI-EPCs visualized by confocal microscopy at 0 and 24 h post-ADSCs-Exos incubation. Scale bars, 10 μm. (E) Fluorescence microscopy analysis was performed to assay the green fluorescent signals in AMI-EPCs co-cultured with ADSCs-Exos with or without GFP-labeled SIRT1 treatment. Scale bars, 10 μm.

ventricular endsystolic dimension (LVESD), and low fractional shortening (FS) and ejection fraction (EF) were significantly enhanced in mice with *CXCR7* deletion compared with WT mice (Figures 5D–5G). *CXCR7* knockout also exacerbated the effects of AMI on the maximal fall and rise of left ventricular pressure (+dP/dt and −dP/dt, respectively) compared with that in $CXCR7^{-/-}$ mice (Figures 5H and 5I). Compared with the PBS control group, the injection of ADSCs-Exos significantly improved the myocardial dysfunction induced by AMI in WT mice, while it did not improve cardiac function in $CXCR7^{-/-}$ mice. These results indicated that *CXCR7* deletion enhanced AMI-induced myocardial dysfunction, suggesting that *CXCR7* may have a protective effect against AMI-induced impairment of cardiovascular function. ADSCs-SIRT1-Exo injection helped restore cardiac function in AMI of WT mice but not in that of $CXCR7^{-/-}$ mice, showing that the presence of *CXCR7* was necessary for the efficacy of ADSC-SIRT1-Exo injection, which was consistent with the results of our *in vitro* experiments.

Injection of Exosomes from ADSCs Overexpressing SIRT1 Reduced AMI-Induced Infarct Size

Failure to inhibit fibrosis and inflammation can lead to poor ventricular remodeling, which eventually leads to heart failure and death. Given the improvement of myocardial function by injection of ADSCs-SIRT1-Exos, we then examined the cardiac structural response to AMI and modified it by injecting ADSCs-SIRT1-Exos. As shown after Masson's trichrome staining, in macro- and micro-images of hearts from WT mice treated with sham or AMI surgery (Figure 6A), a large area of blue collagen deposition was seen in the AMI mice treated by PBS (AMI + vehicle), indicating a severe infarcted myocardium. The AMI hearts treated by injection of ADSCs-Exos or ADSCs-SIRT1-Exos had significantly reduced degrees of fibrosis compared with the PBS group ($p < 0.05$ and $p < 0.01$, respectively). Compared with the ADSCs-Exo group, the injection of ADSCs-SIRT1-Exos was more effective. The quantitative data in Figure 6A show that decreases inthe fibrosis area (Figure 6B) and the infarct size (Figure 6C) were observed in both the ADSCs-Exo and ADSCs-SIRT1-Exo groups, and the ADSCs-SIRT1-Exo group had a more positive effect on the recovery and reconstruction of cardiac function after AMI.

Injection of Exosomes from ADSCs Overexpressing SIRT1 Reduced AMI-Induced Inflammation

The inflammatory response is the first stage of cardiac remodeling and repair after AMI. In this process, macrophages play a key role in the transition between inflammation and repair.[30–32] In our study, myocardial inflammation was assessed by measuring the infiltration of macrophages at 3 and 7 days after AMI. The results showed that the ADSCs-Exo and ADSCs-SIRT1-Exo groups significantly reduced the increases of macrophages at 3 and 7 days after AMI, indicating that ADSCs-Exos and ADSCs-SIRT1-Exos—especially ADSCs-SIRT1-Exos—reduced the myocardial inflammatory response induced by AMI (Figures 7A and 7B). In addition, assessments of the levels of tumor necrosis factor alpha (TNF-α), interleukin (IL)-1β, and IL-10 by enzyme-linked immunosorbent assays (ELISAs) in the heart homogenates from sham mice and AMI mice with the indicated exosome injections at 24 h after surgery showed that ADSCs-Exos and ADSCs-SIRT1-Exos—especially ADSCs-SIRT1-Exos—significantly attenuated the AMI-induced upregulation of TNF-α and IL-1β and the downregulation of IL-10 (Figures 7C–7E). Together, these results suggested that ADSCs-SIRT1-Exos were more capable of regulating ventricular remodeling and inflammatory responses, potentially shifting the balance toward a more favorable outcome.

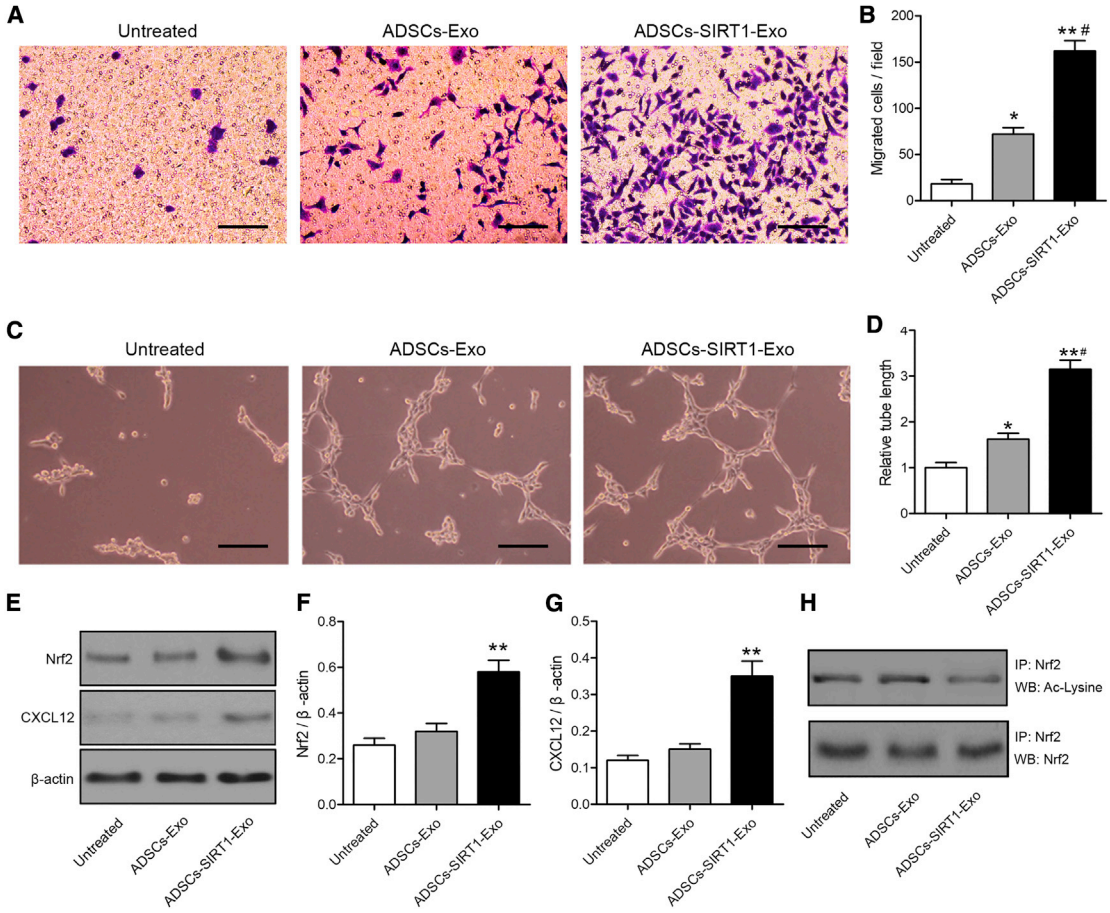

Figure 4. Exosomes from ADSCs Overexpressing SIRT1 Restored AMI-EPC Migration and Tube Formation

(A) Cell migration was measured using Transwell assays. Upper chamber: AMI patient endothelial progenitor cells (EPCs) with or without pretreatment with 200 μg/mL ADSCs-Exos or ADSCs-SIRT1-Exos for 24 h; lower chamber: DMEM containing 10% FBS. Scale bars, 100 μm. (B) The number of migrated cells was calculated. *$p < 0.05$; **$p < 0.01$, compared with the untreated group; #$p < 0.05$, compared with the ADSCs-Exo-treated group. (C–H) EPCs from AMI patients were pretreated with ADSCs-Exos or ADSCs-SIRT1-Exos for 24 h. (C) Tube formation assay. Scale bars, 100 μm. (D) The tube lengths were measured. The AMI-EPCs without any treatment were normalized to 1. *$p < 0.05$; **$p < 0.01$, compared with the untreated group; #$p < 0.05$, compared with the ADSCs-Exos-treated group. (E) Expressions of Nrf2 and CXCL12 in AMI-EPCs were detected by western blotting. (F and G) The western blot results were normalized to β-actin; (F) Nrf2 and (G) CXCL12. **$p < 0.01$, compared with the untreated group. (H) Acetylated Nrf2 levels were measured by immunoprecipitation.

Injection of Exosomes from ADSCs Overexpressing SIRT1 Induced Vasculogenesis

Finally, we assessed the effect of ADSCs-SIRT1-Exos on angiogenesis. We performed immunofluorescent staining for α-smooth muscle actin (α-SMA) or von Willebrand factor (vWF), which served as markers of mature new blood vessels in peri-infarcted myocardium at 28 days post-AMI (Figure 8). Regarding the density of arterioles (α-SMA + vessels), a significantly greater number of arterioles in WT mice was observed in the ADSCs-Exo and ADSC-SIRT1-Exo injection groups when compared to the sham or PBS control group (vehicle), and the highest expression of α-SMA was observed in the ADSC-SIRT1-Exo group, suggesting the recovery of myocardial injury after AMI. No statistical difference was found among all the knockout mice (Figures 8A and 8B). The vWF is mainly derived from vascular endothelial cells and plays an important role in regulating platelet adhesion to the vessel wall. As shown in Figures 8C and 8D, the trend of vWF staining was similar to that of α-SMA, indicating the ability of ADSCs-SIRT1-Exos to induce beneficial angiogenesis for infarcted myocardium. Together, these findings suggested that ADSC-SIRT1-Exos had the greatest effect on angiogenesis but that the effect was blocked after CXCR7 knockout.

DISCUSSION

AMI is a disease with high worldwide mortality and morbidity. Although more than a decade of clinical trials has been conducted on stem cell transplantation for the treatment of cardiovascular diseases, there has been no major breakthrough in treatment efficacy.[33] The main reason may be the lack of a blood supply to the infarction myocardium, leading to a conservative therapeutic effect for AMI treatments. Angiogenesis is a physiological process involving the

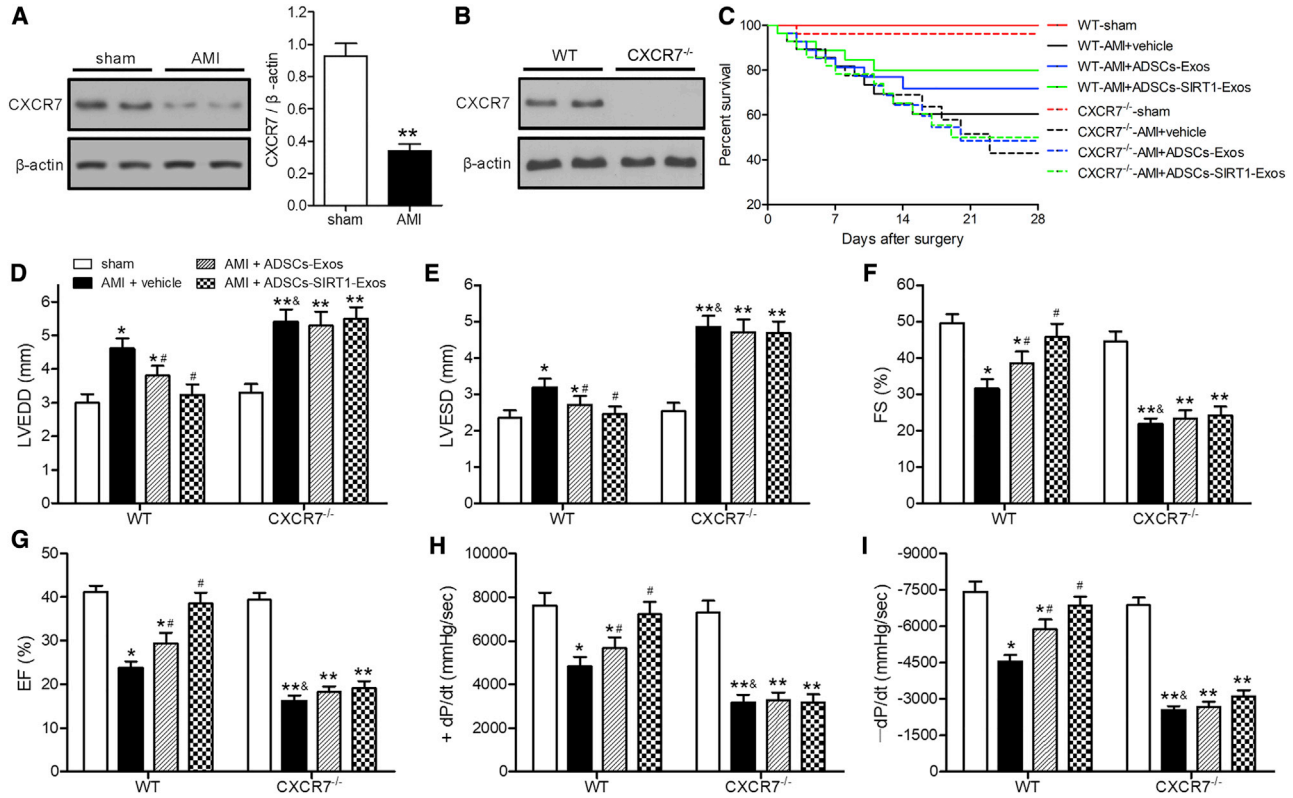

Figure 5. Injection of Exosomes from ADSCs Overexpressing SIRT1 Helped Restore Cardiac Function in AMI of WT mice but Not in *CXCR7*$^{-/-}$ Mice

AMI was produced by surgical ligation of the left anterior descending (LAD) coronary artery. LAD artery ligation or sham surgery was performed in mice; injection of phosphate-buffered saline (PBS; vehicle), ADSCs-Exos, or ADSCs-SIRT1-Exos was performed after AMI surgery, and myocardial tissue samples were collected at 28 days after surgery. (A and B) Western blot analyses of the expression levels of CXCR7. The CXCR7 levels were normalized to β-actin. *$p < 0.05$, compared with the sham group. (C) Survival analysis of mice treated as indicated each day after surgery. (D–I) Echocardiographic and hemodynamic measurements of the left ventricular enddiastolic dimension (LVEDD) (D); left ventricular endsystolic dimension (LVESD) (E); fractional shortening (FS) (F); ejection fraction (EF) (G); rates of maximal rise in left ventricular pressure (+dP/dt) (H); and the rate of maximal fall in left ventricular pressure (−dP/dt) (I). *$p < 0.05$; **$p < 0.01$, compared with the sham group; $^{\#}p < 0.05$, compared with the AMI + vehicle group of WT mice; $^{\&}p < 0.05$, compared with the AMI + vehicle group of WT mice; n = 6 per group.

formation of new blood vessels from existing blood vessels, which is manifested as the proliferation, migration, and tube formation of endothelial cells. In AMI patients, the number of EPCs decreases, and endothelial dysfunction and local angiogenesis are impaired.[34] We, therefore, need to promote vascular formation and repair the damaged myocardial function.

In the present study, we showed that CXCR7 was significantly downregulated and EPCs were dysfunctional in peripheral blood from AMI patients. To decrease the dysfunction of AMI-EPCs, ADSCs were selected. A large number of ADSCs can be obtained by liposuction, and 2,500 times more can be isolated from bone marrow mesenchymal stem cells (BMSCs) isolated from fresh bone marrow.[35,36] Clinical trials on AMI patients treated with ADSC injections have shown that ADSCs are safe and feasible for the treatment of AMI, which is specifically manifested as improved cardiac function, significantly reduced myocardial infarction area, and decreased myocardial fibrosis.[37] However, due to excessive inflammatory reactions and oxidative stress, aging and low survival rates limit the effectiveness of ADSCs in tissue repair and limit the optimal effect of cell therapy. Exosomes are membrane vesicles with a diameter of 80–120 nm and are secreted by a variety of cells and distributed widely in body fluids, containing proteins, lipids, nucleic acids, etc.[9,10,38] Studies have shown that the role of exosomes is very extensive, involving cell signaling, cell differentiation, immune regulation, substance metabolism, gene regulation, and tumor cell growth.[39–41]

Studies have shown that SIRT1 can protect human umbilical-cord-derived fibroblasts from senescence induced by *in vitro* subculture by promoting telomerase reverse transcriptase transcription.[42] Yuan *et al.*[43] found that SIRT1 improved the senescence of young MSCs during *in vitro* subculturing. Studies have also reported that SIRT1 prevents cardiovascular aging and vascular wall dysfunction by promoting the homeostasis mechanism of antioxidative stress.[44,45] Doulamis *et al.*[46] reported that the combined effects of low SIRT1 and high MMP2 were significantly correlated with AMI.

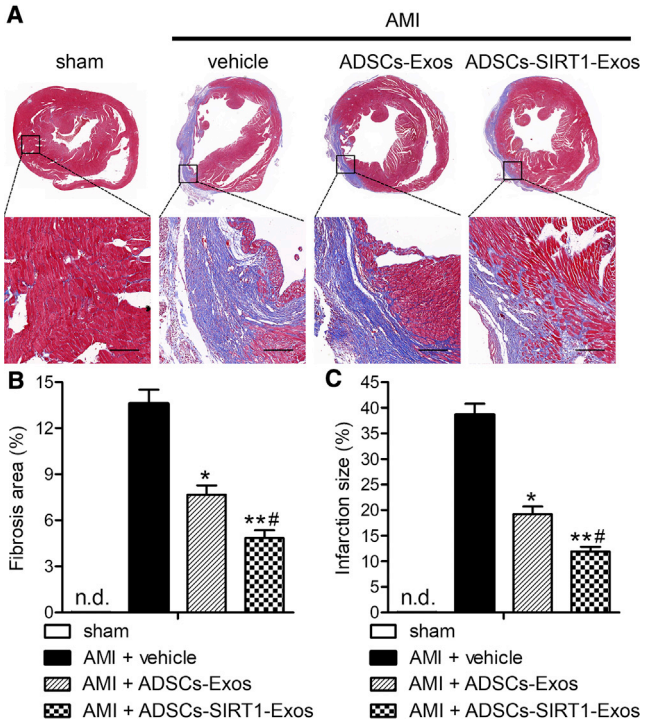

Figure 6. Injection of Exosomes from ADSCs Overexpressing SIRT1 Reduced the Infarct Size and Post-AMI Left Ventricular Remodeling

(A) Cardiac structures in the groups as revealed by Masson's trichrome straining. Scale bars, 100 μm. (B and C) Quantitative analysis of the fibrosis area (B) and infarct size (C). *$p < 0.05$; **$p < 0.01$, compared with the AMI + vehicle group; #$p < 0.05$, compared with the AMI + ADSCs-Exo group; n = 6 per group. n.d., not determined.

Our study showed that exosomes from ADSCs overexpressing SIRT1 positively regulated the expression levels of Nrf2 and chemokine CXCL12 in AMI-EPCs. In addition, functional and morphological studies showed that ADSCs-SIRT1-Exos reduced AMI-induced myocardial fibrosis and inflammation responses and promoted angiogenesis in mice. Secretions of TNF-α, IL-1β, and IL-10 are associated with the Th17 and Th9 subsets of T helper cells, which are recruited to the heart post-AMI.[47,48] Nrf2 is a widely expressed transcription factor, and the SIRT1/Nrf2 signaling pathway plays an important role in oxidative stress.[49] Wang et al.[22] reported that activation of the SIRT1/Nrf2 signaling pathway reduced myocardial ischemia/reperfusion injury. Qiu et al.[50] showed that CXCL12 upregulation played an anti-inflammatory and anti-apoptotic role in improving myocardial function. A potential mechanism involves SIRT1 enhancing the function of EPCs and, ultimately, improving the myocardial function of AMI mice, which may be related to the activation of Nrf2 and the upregulation of CXCL12. After AMI, the regeneration ability of the heart is limited, leading to fibrosis of myocardial tissue, which leads to impaired myocardial function.[51] Increasing vascular density is an effective method to restore blood flow in ischemic regions through angiogenesis.[52]

CXCR7 is necessary for the regulation of various cellular functions,[53] and it is a receptor with a strong affinity for CXCL12.[27] It has been reported that CXCR7 plays a key role in the adhesion and survival regulation of EPCs from both rat bone marrow and human umbilical cord blood.[54,55] Our results showed that ADSC-SIRT1-Exos promoted AMI-EPC migration and tube formation, which may be due to increased CXCL12 by ADSCs-SIRT1-Exos and its subsequent binding to the receptor CXCR7. This study also found that the overexpression of CXCR7 saved the impaired function of AMI-EPCs, indicating that the upregulation of CXCR7 restored angiogenesis. In contrast, downregulation of CXCR7 resulted in impaired EPC function in healthy subjects, and CXCR7 knockout completely disrupted the effect of ADSC-SIRT1-Exos on improving myocardial function in AMI mice. These results confirmed that CXCR7 played an important role in the function of EPCs.

In conclusion, we have provided convincing evidence for the mechanism of cardiac functional repair in AMI by injecting ADSC-SIRT1-Exos (Figure 8). First, we found that the expression level of CXCR7 was closely related to EPC functioning in AMI, which was manifested as the downregulation of CXCR7 levels in AMI-EPCs and myocardial tissue of AMI mice. Downregulation of CXCR7 in control-EPCs caused EPC dysfunction, while overexpression of CXCR7 in AMI-EPCs restored EPC function. Second, we found that ADSCs-SIRT1-Exos promoted the migration and tube formation of AMI-EPCs and that ADSCs-SIRT1-Exo injection improved heart function and reduced the infarct area. Finally, we found that the myocardial repair function of ADSCs-SIRT1-Exos involved the activation of Nrf2 and the existence of a CXCL12/CXCR7 axis. This study may provide new ideas for the treatment of AMI.

MATERIALS AND METHODS

Patients

Peripheral blood mononuclear cells were collected from patients with AMI (n = 65) and healthy controls (n = 38) at Shanghai Gongli Hospital (Shanghai, China) between January 2016 and December 2017. Characteristics of patients and healthy control subjects are presented in Table 1. Patients with previous AMI or coronary artery bypass surgery, previous severe heart valvular disease, acute or chronic liver disease, and elevated serum creatinine levels on admission were excluded. None of the patients in the study had been treated with statins, and none had systemic inflammation or malignancies. All participants were informed of the purpose of the study and gave written informed consent. The study adhered to the Declaration of Helsinki regarding the use of human blood and was approved by the local ethics committee.

Isolation and Culture of EPCs

EPCs were obtained and cultured as previously described.[56] Briefly, 20 mL peripheral blood was collected immediately after admission. Peripheral blood from healthy subjects was used as the control group. Peripheral blood mononuclear cells were isolated using density gradient centrifugation and then inoculated at 5×10^5/cm into fibronectin-coated, 6-well plates in Endothelial Basal Medium-2 (HyClone, Logan City, UT, USA) containing 20% fetal bovine serum (FBS; GIBCO, Grand Island, NY, USA), vascular endothelial growth

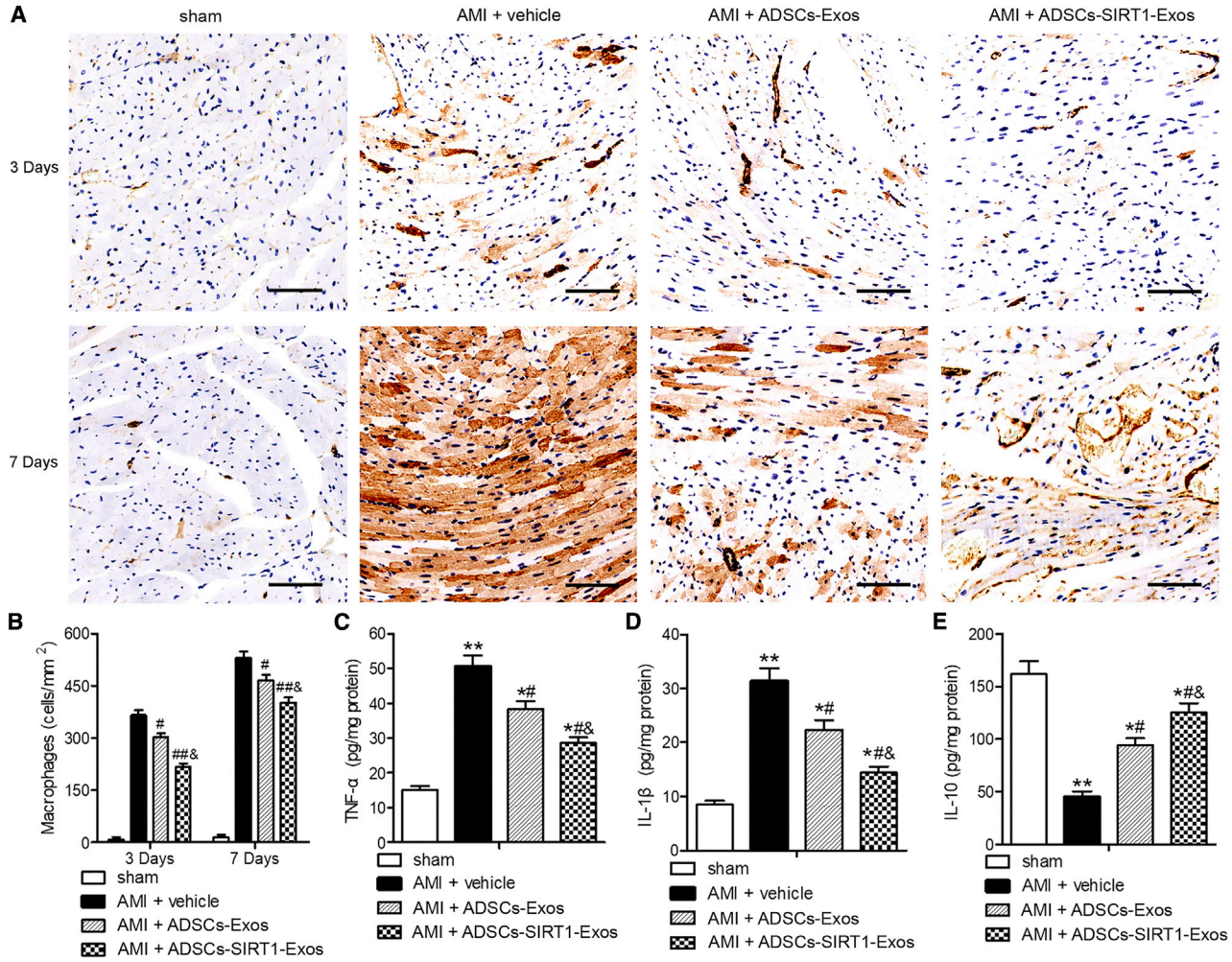

Figure 7. Injection of Exosomes from ADSCs Overexpressing SIRT1 Decreased AMI-Induced Myocardial Inflammation

(A) Macrophage density was assessed using Mac3 staining. Scale bars, 100 μm. (B) Quantification of infiltrated macrophages per area in frozen sections of infarcted hearts at days 3 and 7 after AMI surgery. $^{\#}p < 0.05$; $^{\#\#}p < 0.01$, compared with the AMI + vehicle group; $^{\&}p < 0.05$, compared with the AMI + ADSCs-Exos group; n = 6 per group. (C–E) The levels of TNF-α (C), IL-1β (D), and IL-10 (E) measured in heart homogenates after AMI or sham surgery for 24 h. $^{*}p < 0.05$; $^{**}p < 0.01$, versus the sham group; $^{\#}p < 0.05$, compared with the AMI + vehicle group; $^{\&}p < 0.05$, compared with the AMI + ADSCs-Exos group; n = 6 per group.

factor, insulin-like growth factor, ascorbic acid, heparin, and antibiotics and cultured at 37°C in 5% CO_2. After 4 days of culture, the non-adherent cells were removed with PBS. The adherent cells were cultured for another 3 days before subsequent experiments. EPCs were confirmed by assessing the surface markers CD34, CD133, and CD45 (Abcam, Cambridge, MA, USA) with flow cytometry analyses, and isotype control antibodies were used as negative controls.

Lentiviral Vector Construction and Transfection

To overexpress *SIRT1* in ADSCs and for the overexpression of *CXCR7* in AMI-EPCs, the cDNAs of human SIRT1 and CXCR7 were amplified by PCR using specific primers (SIRT1, forward primer: 5′-AGT CTC GAG TGG AAG ATG GCG GAC GAG-3′, and reverse primer: 5′-CTC GGA TCC TCT CTG GAA CAT CAG GCT C-3′; CXCR7, forward primer: 5′-CGA CTC GAG ATC CTG CTG ACC TCC TAC-3′, and reverse primer: 5′-CCG GGA TCC AAG CTA CTT TGC TTT GCT-3′). The purified PCR product was cloned into pLVX plasmid vector (Clontech, Mountain View, CA, USA) encoding GFP to generate the Lv-*SIRT1* or Lv-*CXCR7* plasmid. For lentiviral production, Lv-*SIRT1* or Lv-*CXCR7* recombinant vectors or control vector with psPAX2 and pMD2, were co-transfected into HEK293T cells. After transfection for 48 h, lentiviral supernatants were collected through a 0.45-μm filter (Millipore, Billerica, MA, USA). ADSCs or AMI-EPCs were infected overnight with the corresponding lentiviral vector (recombinant SIRT1 or CXCR7 or control vector) at a multiplicity of infection (MOI) of 25. At 48 h after transfection, the infection efficiency was determined by western blots.

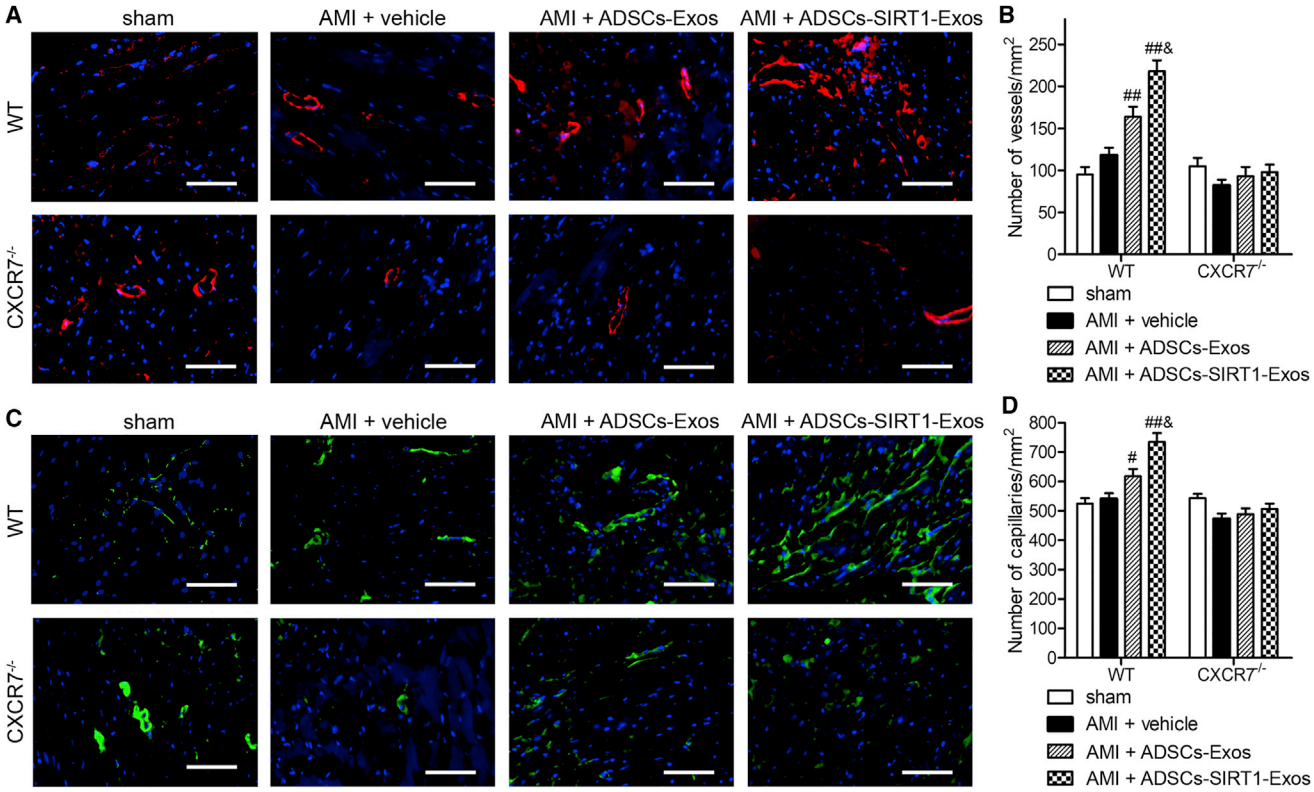

Figure 8. Injection of Exosomes from ADSCs Overexpressing SIRT1-Induced Vasculogenesis

(A and B) Arteriole density from α-SMA staining. Representative images (A, Scale bars, 100 μm.) and quantification (B) of arteriole density in the peri-infarcted myocardium at 28 days after AMI, analyzed by α-SMA staining. $^{\#}p < 0.05$; $^{\#\#}p < 0.01$, compared with the AMI + vehicle group; $^{\&}p < 0.05$, compared with the AMI + ADSCs-Exos group; n = 6 per group. (C and D) Capillary density from vWF-positive vessels; representative images (C, Scale bars, 100 μm.) and quantification (D). The blood vessel density is indicated as the vessel number per square millimeter. $^{\#}p < 0.05$; $^{\#\#}p < 0.01$, compared with the AMI + vehicle group; $^{\&}p < 0.05$, compared with the AMI + ADSCs-Exos group; n = 6 per group.

To knock down *SIRT1* in ADSCs and knock down *CXCR7* in control-EPCs, lentiviruses containing siRNA against *SIRT1*, *CXCR7*, or nonsense siRNA were constructed (si*SIRT1*: 5′-GCG GCT TGA TGG TAA TCA GTA-3′; si*CXCR7*: 5′-CGC TCT CCT TCA TTT ACA TTT-3′; and nonsense siRNA: 5′-CAG CCA TCA ACT CAG ATT GTT-3′) by Hanbio Biotechnology (Shanghai, China). The transfection was performed following the procedure described earlier. After transfection for 48 h, the expression of SIRT1 and CXCR7 was determined by western blot.

Isolation and Identification of Exosomes

Exosomes from ADSCs culture media were extracted by differential centrifugation, as described previously.[38,57] The ultrastructure of the exosomes was visualized using a transmission electron microscope (Libra 120; Zeiss, Oberkochen, Germany). The sizes of exosomes were directly tracked using nanoparticle tracking analysis using a Nanosight LM10 (Malvern Instruments, Malvern, UK) and the results were analyzed with NTA v.3.0 software (Malvern Instruments). Western blotting using antibodies against CD63 and TSG101 (representative markers of exosomes) was used to identify the collected exosomes.

PKH26-Labeled Exosomes and Tracking in EPCs

To track ADSCs-Exos in EPCs, PKH26 (Sigma-Aldrich, St. Louis, MO, USA) and labeled ADSCs-Exos (PKH26-ADSCs-Exos) were added to AMI-EPCs and incubated at 37°C for 24 h. The cells were washed to remove the uninternalized exosomes, and the fluorescent images were visualized using a confocal microscope.

Western Blot Assays

Proteins from exosomes, EPCs, ADSCs and mouse myocardial tissues were extracted by using lysates. The bicinchoninic acid (BCA) assay kit (Beyotime Institute of Biotechnology, Jiangsu, China) was used to determine the protein concentration of each sample. Forty micrograms of total protein was separated by 10% SDS-PAGE and transferred to nitrocellulose membranes (Millipore, Jaffrey, NH, USA). After blocking in 5% nonfat milk for 1 h, the membranes were incubated with primary antibodies against CXCR7 (1:500; Abcam), SIRT1 (1:200; Santa Cruz Biotechnology, Santa Cruz, CA, USA), CD63(1:500; Abcam), TSG101(1:500; Abcam), Nrf2 (1:500; Abcam), CXCL12 (1:1,000; Abcam), or β-actin (1:2,000; Abcam) overnight at 4°C. After washing, the membranes were incubated with horseradish peroxidase (HRP)-conjugated

Table 1. Clinical Characteristics of AMI Patients and Healthy Controls Included in the Study

Variable	AMI Patients (n = 65)	Healthy Controls (n = 38)	p
Age in years (mean ± SD)	57.26 ± 9.17	54.31 ± 5.29	0.163
Male, n (%)	35 (53.85)	21 (55.26)	0.511
Body mass index in kg/m^2 (mean ± SD)	26.14 ± 2.45	27.35 ± 1.84	0.347
Smoking, n (%)	33 (50.77)	14 (36.84)	0.209
Hypertension, n (%)	45 (69.23)	13 (34.21)	0.192
Hypercholesterolemia, n (%)	37 (56.92)	10 (26.32)	0.104
Diabetes mellitus, n (%)	8 (12.31)	2 (5.26)	0.095
Family history of CAD, n (%)	11 (16.92)	5 (10.53)	0.218

Data are expressed as the mean ± SD or percentage (%) (n). AMI, acute myocardial infarction; SD, standard deviation; CAD, coronary artery disease, n, number.

secondary antibodies at room temperature for 1 h. The signals were detected using an enhanced chemiluminescence (ECL) detection system (Thermo Scientific, Rockford, IL, USA). The relative protein levels were determined after normalization with β-actin. Densitometric analysis of the bands was performed using ImageJ software (National Institutes of Health, Bethesda, MD, USA).

Detection of Acetylated Nrf2

AMI-EPCs were pretreated with exosomes (200 μg/mL) from ADSCs or SIRT1-overexpressing ADSCs for 24 h, and cell lysates of total proteins were incubated with Nrf2 antibody (1:500) and precipitated with Protein A/G PLUS-Agarose (Santa Cruz Biotechnology, Santa Cruz, CA, USA). Finally, western blotting was performed using anti-acetylated-lysine antibody (1:200; Abcam).

Cell Migration Assay

The migratory ability of EPCs was assessed using a modified Transwell chamber assay as previously described.[58] EPCs from healthy controls transfected with lentiviral siCXCR7 or control siRNA and AMI-EPCs transfected with lentiviral Lv-CXCR7 or control vector were seeded in the upper chambers. DMEM containing 10% FBS was added to the lower chambers, or they were seeded with ADSCs with or without pretreatment with 2.5 μM GW4869 (exosome inhibitor; Sigma-Aldrich) for 8 h. To investigate whether exosomes from ADSCs overexpressing SIRT1 enhanced the migration ability of AMI-EPCs, the upper chambers were seeded with AMI- EPCs pretreated with 200 μg/mL exosomes from ADSCs or SIRT1-overexpressing ADSCs for 24 h. DMEM containing 10% FBS was added to the bottom chambers. After the cells were cultured in Transwell chambers for 24 h, the chambers were washed with PBS to remove non-migrating EPCs. Migrating cells were fixed by 4% paraformaldehyde and stained with hematoxylin. The numbers of migrated cells on the lower side of the membrane were counted in 10 random high-power fields using an inverted light microscope (Leica DMIL, Wetzlar, Germany).

Tube Formation Assay

A Matrigel basement membrane matrix (Trevigen, Gaithersburg, MD, USA) was placed in a 24-well cell-culture plate, and 1×10^4 EPCs with indicated transfections were added to the wells containing supernatants of ADSCs with or without pretreatment with GW4869. To determine whether ADSCs-SIRT1-Exos promoted the angiogenesis of AMI-EPCs, AMI-EPCs were pretreated with exosomes from ADSCs or SIRT1-overexpressing ADSCs for 24 h. After another 48 h of incubation, tube structures were observed with an inverted microscope (Leica). The tube lengths were measured in 10 random fields per sample by investigators who were unaware of the study's purpose.

Mouse AMI Model and Exosome Injection

All animal experiments were performed in accordance with the Chinese legislation on the use and care of laboratory animals and were approved by the Institutional Animal Care and Utilization Committee of Shanghai Pudong New Area Gongli Hospital. WT and *CXCR7* knockout (*CXCR7*$^{-/-}$) C57BL/6J littermate male mice, 8 weeks old, were purchased from The Jackson Laboratory (Bar Harbor, ME, USA). A mouse AMI model was established by left anterior descending (LAD) coronary artery ligation as described previously.[59] Briefly, mice were injected intraperitoneally with ketamine (50 mg/kg) for anesthesia. The LAD artery was ligated using a silk suture at 1–2 mm between the left side of the pulmonary conus and the right side of the left atrial appendage, and then the heart was put back into the chest, and the incision was sutured. The sham-surgery mice underwent the same procedure without a coronary artery ligation and served as controls.

WT and *CXCR7*$^{-/-}$ mice were randomly assigned to four groups as follows: the sham group (n = 8 for each time point of WT and *CXCR7*$^{-/-}$), in which mice received a sham operation; the AMI + vehicle group (n = 12 for each time point of WT and CXCR7$^{-/-}$), in which mice suffering AMI received a intra-myocardial injection of PBS; the AMI + ADSCs-Exo group (n = 12 for each time point of WT and *CXCR7*$^{-/-}$), in which mice suffering AMI received an intra-myocardial injection of exosomes from ADSCs; and the AMI + ADSCs-SIRT1-Exo group (n = 12 for each time point of WT and *CXCR7*$^{-/-}$), in which mice suffering AMI received an intra-myocardial injection of exosomes from ADSCs infected with SIRT1-overexpressed lentivirus. Exosome injection was performed at 1 h after induction of AMI and then once a week. Exosomes (100 μg protein) in 20 μL PBS were myocardially injected near the ligation site in the free wall of the left ventricle.[60] Survival analysis was performed by daily cage inspection for up to 28 days after surgery.

Echocardiographic and Hemodynamic Measurements

Echocardiography (Vevo 2100 imaging system; Vevo 2100, VisualSonics, Toronto, ON, Canada) was used to examine the cardiac function of mice after surgery for 28 days. The echocardiography parameters were recorded in mice anesthetized with ketamine. Echocardiography parameters included LVEDD, LVESD, left ventricular FS, and left ventricular EF. For hemodynamic measurements, the tip of the left ventricle was punctured, and a miller catheter connected

to the pressure sensor was inserted. +dP/dt and −dP/dt of left ventricular pressure were recorded. The researchers were unaware of the treatment assignment when performing and reading echocardiography and hemodynamic parameters.

Histology and Immunohistochemistry

Some mice were euthanized at 3 or 7 days after surgery, and others were euthanized at 28 days after echocardiography and hemodynamic measurements. The hearts were cut into three transverse sections, fixed at 4°C with 4% paraformaldehyde, dehydrated in a graded series of ethanol, and then embedded in paraffin. Sections were sliced into 10-μm-thick slices and were stained with Masson's trichrome. ImageJ software was used to quantitate the fibrotic area and the size of the infarct area. The percentage of fibrotic area was the ratio of the fibrotic area to the area of the entire high-power field image. The infarct size was calculated by averaging the percentage of the concentrated area near the midsection of the infarct tissue.

For immunofluorescence staining overnight, the sections were incubated overnight at 4°C with antibodies to α-SMA (1:200) or vWF (1:200) (Abcam). After washing with PBS three times, the sections were incubated with secondary antibodies for 2 h at 4°C, then with DAPI staining for 2 min, and examined using a fluorescence microscope.

For immunohistochemistry analyses, macrophages were detected by using Mac3 antibody (1:200; Abcam). The quantitative assessment of macrophage density was done by double-blind counting of Mac3 immunoreactive cells in five different regions of the infarct area. Images were captured using an inverted microscope.

ELISA Analysis

To detect TNF-α, IL-1β, and IL-10 levels in mouse hearts, myocardial tissues from sham mice and AMI mice with the indicated ADSCs-exosome injection at 24 h after surgery were homogenized in PBS buffer. Total protein was extracted with a protein extraction kit (Beyotime). Levels of TNF-α, IL-1β, and IL-10 in heart homogenates were measured with an ELISA kit (R&D Systems), according to the manufacturer's instructions. The results were expressed as protein in picograms per milligram.

Statistical Analysis

Results are expressed in the mean ± SEM from at least three separate experiments. All data were verified for normal distribution. All statistical analyses were performed using GraphPad Prism-5 software. One-way analysis of variance (ANOVA) followed by Tukey's post hoc test was applied to determine the significance among groups. Student's t test was used for statistical analysis to investigate whether there was a significant difference in between groups. $p < 0.05$ was considered statistically significant.

SUPPLEMENTAL INFORMATION

Supplemental Information can be found online at https://doi.org/10.1016/j.omtn.2020.07.007.

AUTHOR CONTRIBUTIONS

H.H. and Z.X. conceived the experiments. H.H. and H.W. wrote the manuscript. Z.X., Y.Q., and W.Z. conducted the experiments. H.H., Z.X., and C.Z. analyzed the data. M.J., S.D., and H.W. contributed reagents. All authors read and approved the final manuscript.

CONFLICTS OF INTEREST

The authors declare no competing interests.

ACKNOWLEDGMENTS

This study was funded by the Featured Special Disease Fund of Pudong New District (grant PWZzb2017-27 to H.W.); the Fund of Shanghai Municipal Commission of Health and Family Planning (grant 201740307 to H.W.); the Science and Technology Development Fund of Pudong New District Minsheng Scientific Research (Medical and Health) Project (grant PKJ2017-Y24 to M.J.); and The National Natural Science Foundation of China (no. 81700428 to S.D.).

REFERENCES

1. Benjamin, E.J., Virani, S.S., Callaway, C.W., Chamberlain, A.M., Chang, A.R., Cheng, S., Chiuve, S.E., Cushman, M., Delling, F.N., Deo, R., et al.; American Heart Association Council on Epidemiology and Prevention Statistics Committee and Stroke Statistics Subcommittee (2018). Heart Disease and Stroke Statistics-2018 Update: A Report From the American Heart Association. Circulation *137*, e67–e492.

2. Lee, T.M., Harn, H.J., Chiou, T.W., Chuang, M.H., Chen, C.H., Lin, P.C., and Lin, S.Z. (2017). Targeting the pathway of GSK-3β/nerve growth factor to attenuate post-infarction arrhythmias by preconditioned adipose-derived stem cells. J. Mol. Cell. Cardiol. *104*, 17–30.

3. Toma, C., Pittenger, M.F., Cahill, K.S., Byrne, B.J., and Kessler, P.D. (2002). Human mesenchymal stem cells differentiate to a cardiomyocyte phenotype in the adult murine heart. Circulation *105*, 93–98.

4. Amado, L.C., Saliaris, A.P., Schuleri, K.H., St John, M., Xie, J.S., Cattaneo, S., Durand, D.J., Fitton, T., Kuang, J.Q., Stewart, G., et al. (2005). Cardiac repair with intramyocardial injection of allogeneic mesenchymal stem cells after myocardial infarction. Proc. Natl. Acad. Sci. USA *102*, 11474–11479.

5. McGinley, L.M., McMahon, J., Stocca, A., Duffy, A., Flynn, A., O'Toole, D., and O'Brien, T. (2013). Mesenchymal stem cell survival in the infarcted heart is enhanced by lentivirus vector-mediated heat shock protein 27 expression. Hum. Gene Ther. *24*, 840–851.

6. Li, L., Chen, X., Wang, W.E., and Zeng, C. (2016). How to Improve the Survival of Transplanted Mesenchymal Stem Cell in Ischemic Heart? Stem Cells Int. *2016*, 9682757.

7. Pan, W., Zhu, Y., Meng, X., Zhang, C., Yang, Y., and Bei, Y. (2019). Immunomodulation by Exosomes in Myocardial Infarction. J. Cardiovasc. Transl. Res. *12*, 28–36.

8. Liu, Z., Xu, Y., Wan, Y., Gao, J., Chu, Y., and Li, J. (2019). Exosomes from adipose-derived mesenchymal stem cells prevent cardiomyocyte apoptosis induced by oxidative stress. Cell Death Discov. *5*, 79.

9. Kordelas, L., Rebmann, V., Ludwig, A.K., Radtke, S., Ruesing, J., Doeppner, T.R., Epple, M., Horn, P.A., Beelen, D.W., and Giebel, B. (2014). MSC-derived exosomes: a novel tool to treat therapy-refractory graft-versus-host disease. Leukemia *28*, 970–973.

10. Sharma, A. (2018). Role of stem cell derived exosomes in tumor biology. Int. J. Cancer *142*, 1086–1092.

11. Kong, F.L., Wang, X.P., Li, Y.N., and Wang, H.X. (2018). The role of exosomes derived from cerebrospinal fluid of spinal cord injury in neuron proliferation in vitro. Artif. Cells Nanomed. Biotechnol. *46*, 200–205.

12. Xu, H., Wang, Z., Liu, L., Zhang, B., and Li, B. (2020). Exosomes derived from adipose tissue, bone marrow, and umbilical cord blood for cardioprotection after myocardial infarction. J. Cell. Biochem. *121*, 2089–2102.

13. Kitada, M., Ogura, Y., and Koya, D. (2016). The protective role of Sirt1 in vascular tissue: its relationship to vascular aging and atherosclerosis. Aging (Albany NY) *8*, 2290–2307.

14. Wang, G., Wang, F., Ren, J., Qiu, Y., Zhang, W., Gao, S., Yang, D., Wang, Z., Liang, A., Gao, Z., et al. (2018). SIRT1 Involved in the Regulation of Alternative Splicing Affects the DNA Damage Response in Neural Stem Cells. Cell. Physiol. Biochem. *48*, 657–669.

15. Zullo, A., Simone, E., Grimaldi, M., Musto, V., and Mancini, F.P. (2018). Sirtuins as Mediator of the Anti-Ageing Effects of Calorie Restriction in Skeletal and Cardiac Muscle. Int. J. Mol. Sci. *19*, 928.

16. Wątroba, M., and Szukiewicz, D. (2016). The role of sirtuins in aging and age-related diseases. Adv. Med. Sci. *61*, 52–62.

17. Ding, M., Lei, J., Han, H., Li, W., Qu, Y., Fu, E., Fu, F., and Wang, X. (2015). SIRT1 protects against myocardial ischemia-reperfusion injury via activating eNOS in diabetic rats. Cardiovasc. Diabetol. *14*, 143.

18. Wang, H., Lv, C., Gu, Y., Li, Q., Xie, L., Zhang, H., Miao, D., and Sun, W. (2018). Overexpressed Sirt1 in MSCs Promotes Dentin Formation in Bmi1-Deficient Mice. J. Dent. Res. *97*, 1365–1373.

19. Sun, W., Qiao, W., Zhou, B., Hu, Z., Yan, Q., Wu, J., Wang, R., Zhang, Q., and Miao, D. (2018). Overexpression of Sirt1 in mesenchymal stem cells protects against bone loss in mice by FOXO3a deacetylation and oxidative stress inhibition. Metabolism *88*, 61–71.

20. Han, D., Huang, W., Li, X., Gao, L., Su, T., Li, X., Ma, S., Liu, T., Li, C., Chen, J., et al. (2016). Melatonin facilitates adipose-derived mesenchymal stem cells to repair the murine infarcted heart via the SIRT1 signaling pathway. J. Pineal Res. *60*, 178–192.

21. Emamgholipour, S., Hossein-Nezhad, A., Sahraian, M.A., Askarisadr, F., and Ansari, M. (2016). Evidence for possible role of melatonin in reducing oxidative stress in multiple sclerosis through its effect on SIRT1 and antioxidant enzymes. Life Sci. *145*, 34–41.

22. Wang, X., Yuan, B., Cheng, B., Liu, Y., Zhang, B., Wang, X., Lin, X., Yang, B., and Gong, G. (2019). Crocin Alleviates Myocardial Ischemia/Reperfusion-Induced Endoplasmic Reticulum Stress Via Regulation of MIR-34A/SIRT1/NRF2 Pathway. Shock *51*, 123–130.

23. Oh, I.Y., Yoon, C.H., Hur, J., Kim, J.H., Kim, T.Y., Lee, C.S., Park, K.W., Chae, I.H., Oh, B.H., Park, Y.B., and Kim, H.S. (2007). Involvement of E-selectin in recruitment of endothelial progenitor cells and angiogenesis in ischemic muscle. Blood *110*, 3891–3899.

24. Regueiro, A., Cuadrado-Godia, E., Bueno-Betí, C., Diaz-Ricart, M., Oliveras, A., Novella, S., Gené, G.G., Jung, C., Subirana, I., Ortiz-Pérez, J.T., et al. (2015). Mobilization of endothelial progenitor cells in acute cardiovascular events in the PROCELL study: time-course after acute myocardial infarction and stroke. J. Mol. Cell. Cardiol. *80*, 146–155.

25. Fish, K.M., Ishikawa, K., and Hajjar, R.J. (2018). Stem cell therapy for acute myocardial infarction: on the horizon or still a dream? Coron. Artery Dis. *29*, 89–91.

26. Rosenkranz, K., Kumbruch, S., Lebermann, K., Marschner, K., Jensen, A., Dermietzel, R., and Meier, C. (2010). The chemokine SDF-1/CXCL12 contributes to the 'homing' of umbilical cord blood cells to a hypoxic-ischemic lesion in the rat brain. J. Neurosci. Res. *88*, 1223–1233.

27. Balabanian, K., Lagane, B., Infantino, S., Chow, K.Y., Harriague, J., Moepps, B., Arenzana-Seisdedos, F., Thelen, M., and Bachelerie, F. (2005). The chemokine SDF-1/CXCL12 binds to and signals through the orphan receptor RDC1 in T lymphocytes. J. Biol. Chem. *280*, 35760–35766.

28. Zhang, X.Y., Su, C., Cao, Z., Xu, S.Y., Xia, W.H., Xie, W.L., Chen, L., Yu, B.B., Zhang, B., Wang, Y., and Tao, J. (2014). CXCR7 upregulation is required for early endothelial progenitor cell-mediated endothelial repair in patients with hypertension. Hypertension *63*, 383–389.

29. Dai, X., Yan, X., Zeng, J., Chen, J., Wang, Y., Chen, J., Li, Y., Barati, M.T., Wintergerst, K.A., Pan, K., et al. (2017). Elevating CXCR7 Improves Angiogenic Function of EPCs via Akt/GSK-3β/Fyn-Mediated Nrf2 Activation in Diabetic Limb Ischemia. Circ. Res. *120*, e7–e23.

30. Ducharme, A., Frantz, S., Aikawa, M., Rabkin, E., Lindsey, M., Rohde, L.E., Schoen, F.J., Kelly, R.A., Werb, Z., Libby, P., and Lee, R.T. (2000). Targeted deletion of matrix metalloproteinase-9 attenuates left ventricular enlargement and collagen accumulation after experimental myocardial infarction. J. Clin. Invest. *106*, 55–62.

31. Yap, J., Cabrera-Fuentes, H.A., Irei, J., Hausenloy, D.J., and Boisvert, W.A. (2019). Role of Macrophages in Cardioprotection. Int. J. Mol. Sci. *20*, 2474.

32. Li, J., Cai, S.X., He, Q., Zhang, H., Friedberg, D., Wang, F., and Redington, A.N. (2018). Intravenous miR-144 reduces left ventricular remodeling after myocardial infarction. Basic Res. Cardiol. *113*, 36.

33. Makkar, R.R., Smith, R.R., Cheng, K., Malliaras, K., Thomson, L.E., Berman, D., Czer, L.S., Marbán, L., Mendizabal, A., Johnston, P.V., et al. (2012). Intracoronary cardiosphere-derived cells for heart regeneration after myocardial infarction (CADUCEUS): a prospective, randomised phase 1 trial. Lancet *379*, 895–904.

34. Yoshioka, K., Yoshida, K., Cui, H., Wakayama, T., Takuwa, N., Okamoto, Y., Du, W., Qi, X., Asanuma, K., Sugihara, K., et al. (2012). Endothelial PI3K-C2α, a class II PI3K, has an essential role in angiogenesis and vascular barrier function. Nat. Med. *18*, 1560–1569.

35. Doppler, S.A., Deutsch, M.A., Lange, R., and Krane, M. (2013). Cardiac regeneration: current therapies-future concepts. J. Thorac. Dis. *5*, 683–697.

36. Kochegarov, A., and Lemanski, L.F. (2016). New Trends in Heart Regeneration: A Review. J. Stem Cells Regen. Med. *12*, 61–68.

37. Houtgraaf, J.H., den Dekker, W.K., van Dalen, B.M., Springeling, T., de Jong, R., van Geuns, R.J., Geleijnse, M.L., Fernandez-Aviles, F., Zijlsta, F., Serruys, P.W., and Duckers, H.J. (2012). First experience in humans using adipose tissue-derived regenerative cells in the treatment of patients with ST-segment elevation myocardial infarction. J. Am. Coll. Cardiol. *59*, 539–540.

38. Liu, J., Jiang, M., Deng, S., Lu, J., Huang, H., Zhang, Y., Gong, P., Shen, X., Ruan, H., Jin, M., and Wang, H. (2018). miR-93-5p-Containing Exosomes Treatment Attenuates Acute Myocardial Infarction-Induced Myocardial Damage. Mol. Ther. Nucleic Acids *11*, 103–115.

39. Schneider, A., and Simons, M. (2013). Exosomes: vesicular carriers for intercellular communication in neurodegenerative disorders. Cell Tissue Res. *352*, 33–47.

40. Lai, R.C., Chen, T.S., and Lim, S.K. (2011). Mesenchymal stem cell exosome: a novel stem cell-based therapy for cardiovascular disease. Regen. Med. *6*, 481–492.

41. Tan, A., Rajadas, J., and Seifalian, A.M. (2013). Exosomes as nano-theranostic delivery platforms for gene therapy. Adv. Drug Deliv. Rev. *65*, 357–367.

42. Yamashita, S., Ogawa, K., Ikei, T., Udono, M., Fujiki, T., and Katakura, Y. (2012). SIRT1 prevents replicative senescence of normal human umbilical cord fibroblast through potentiating the transcription of human telomerase reverse transcriptase gene. Biochem. Biophys. Res. Commun. *417*, 630–634.

43. Yuan, H.F., Zhai, C., Yan, X.L., Zhao, D.D., Wang, J.X., Zeng, Q., Chen, L., Nan, X., He, L.J., Li, S.T., et al. (2012). SIRT1 is required for long-term growth of human mesenchymal stem cells. J. Mol. Med. (Berl.) *90*, 389–400.

44. Cencioni, C., Spallotta, F., Mai, A., Martelli, F., Farsetti, A., Zeiher, A.M., and Gaetano, C. (2015). Sirtuin function in aging heart and vessels. J. Mol. Cell. Cardiol. *83*, 55–61.

45. Kane, A.E., and Sinclair, D.A. (2018). Sirtuins and NAD^+ in the Development and Treatment of Metabolic and Cardiovascular Diseases. Circ. Res. *123*, 868–885.

46. Doulamis, I.P., Tzani, A.I., Konstantopoulos, P.S., Samanidis, G., Georgiopoulos, G., Toutouzas, K.P., Perrea, D.N., and Perreas, K.G. (2017). A sirtuin 1/MMP2 prognostic index for myocardial infarction in patients with advanced coronary artery disease. Int. J. Cardiol. *230*, 447–453.

47. Latet, S.C., Hoymans, V.Y., Van Herck, P.L., and Vrints, C.J. (2015). The cellular immune system in the post-myocardial infarction repair process. Int. J. Cardiol. *179*, 240–247.

48. Jäger, A., and Kuchroo, V.K. (2010). Effector and regulatory T-cell subsets in autoimmunity and tissue inflammation. Scand. J. Immunol. *72*, 173–184.

49. Xia, X., Qu, B., Li, Y.M., Yang, L.B., Fan, K.X., Zheng, H., Huang, H.-D., Gu, J.-W., Kuang, Y.-Q., and Ma, Y. (2017). NFAT5 protects astrocytes against oxygen-glucose-serum deprivation/restoration damage via the SIRT1/Nrf2 pathway. J. Mol. Neurosci. *61*, 96–104.

50. Qiu, R., Cai, A., Dong, Y., Zhou, Y., Yu, D., Huang, Y., Zheng, D., Rao, S., Feng, Y., and Mai, W. (2012). SDF-1α upregulation by atorvastatin in rats with acute myocardial infarction via nitric oxide production confers anti-inflammatory and anti-apoptotic effects. J. Biomed. Sci. *19*, 99.

51. Mihic, A., Cui, Z., Wu, J., Vlacic, G., Miyagi, Y., Li, S.H., Lu, S., Sung, H.W., Weisel, R.D., and Li, R.K. (2015). A Conductive Polymer Hydrogel Supports Cell Electrical Signaling and Improves Cardiac Function After Implantation into Myocardial Infarct. Circulation *132*, 772–784.

52. Ylä-Herttuala, S., and Baker, A.H. (2017). Cardiovascular Gene Therapy: Past, Present, and Future. Mol. Ther. *25*, 1095–1106.

53. Puchert, M., and Engele, J. (2014). The peculiarities of the SDF-1/CXCL12 system: in some cells, CXCR4 and CXCR7 sing solos, in others, they sing duets. Cell Tissue Res. *355*, 239–253.

54. Yan, X., Cai, S., Xiong, X., Sun, W., Dai, X., Chen, S., Ye, Q., Song, Z., Jiang, Q., and Xu, Z. (2012). Chemokine receptor CXCR7 mediates human endothelial progenitor cells survival, angiogenesis, but not proliferation. J. Cell. Biochem. *113*, 1437–1446.

55. Dai, X., Tan, Y., Cai, S., Xiong, X., Wang, L., Ye, Q., Yan, X., Ma, K., and Cai, L. (2011). The role of CXCR7 on the adhesion, proliferation and angiogenesis of endothelial progenitor cells. J. Cell. Mol. Med. *15*, 1299–1309.

56. Tang, Y., Zhang, Y., Chen, Y., Xiang, Y., and Xie, Y. (2015). Role of the microRNA, miR-206, and its target PIK3C2α in endothelial progenitor cell function – potential link with coronary artery disease. FEBS J. *282*, 3758–3772.

57. Li, X., Xie, X., Lian, W., Shi, R., Han, S., Zhang, H., Lu, L., and Li, M. (2018). Exosomes from adipose-derived stem cells overexpressing Nrf2 accelerate cutaneous wound healing by promoting vascularization in a diabetic foot ulcer rat model. Exp. Mol. Med. *50*, 29.

58. Xu, D.Y., Davis, B.B., Wang, Z.H., Zhao, S.P., Wasti, B., Liu, Z.L., Li, N., Morisseau, C., Chiamvimonvat, N., and Hammock, B.D. (2013). A potent soluble epoxide hydrolase inhibitor, t-AUCB, acts through PPARγ to modulate the function of endothelial progenitor cells from patients with acute myocardial infarction. Int. J. Cardiol. *167*, 1298–1304.

59. Hu, H., Wu, J., Li, D., Zhou, J., Yu, H., and Ma, L. (2018). Knockdown of lncRNA MALAT1 attenuates acute myocardial infarction through miR-320-Pten axis. Biomed. Pharmacother. *106*, 738–746.

60. Chen, Y., Zhao, Y., Chen, W., Xie, L., Zhao, Z.A., Yang, J., Chen, Y., Lei, W., and Shen, Z. (2017). MicroRNA-133 overexpression promotes the therapeutic efficacy of mesenchymal stem cells on acute myocardial infarction. Stem Cell Res. Ther. *8*, 268.